Supporting Information
for

Carbon-Coated Ni_3Sn_2 Nanoparticles Embedded in Porous Carbon Nanosheets as Lithium Ion Battery Anode with Outstanding Cycling Stability

Jian Qin [a], Xiang Zhang [a], Naiqin Zhao [a, b], Chunsheng Shi [a], Enzuo Liu [a], Jiajun Li [a], and Chunnian He [a, b, *]

[a]*School of Materials Science and Engineering and Tianjin Key Laboratory of Composites and Functional Materials, Tianjin University, Tianjin 300072, China*

[b]*Collaborative Innovation Center of Chemical Science and Engineering, Tianjin 300072, China*

---

[a] *School of Materials Science and Engineering and Tianjin Key Laboratory of Composites and Functional Materials, Tianjin University, Tianjin 300072, China*

[b] *Collaborative Innovation Center of Chemical Science and Engineering, Tianjin 300072, China*
Email: cnhe08@tju.edu.cn

† Electronic supplementary information (ESI) available.

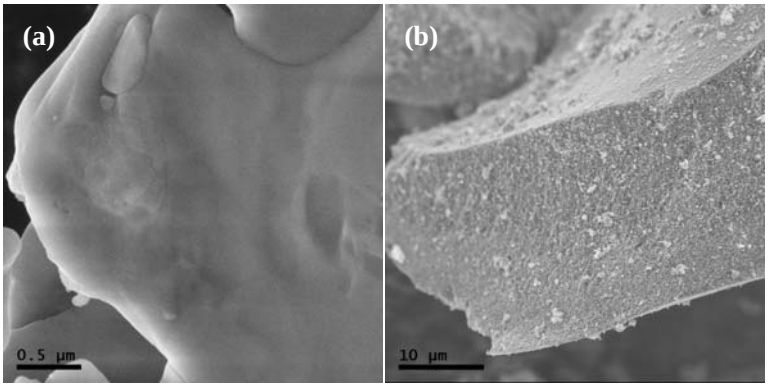

Figure S1. (a) SEM image of $Ni(NO_3)_2$-citric acid complex film coated on the surface of NaCl particles, (b) SEM image of Ni@C@PGC without removing NaCl.

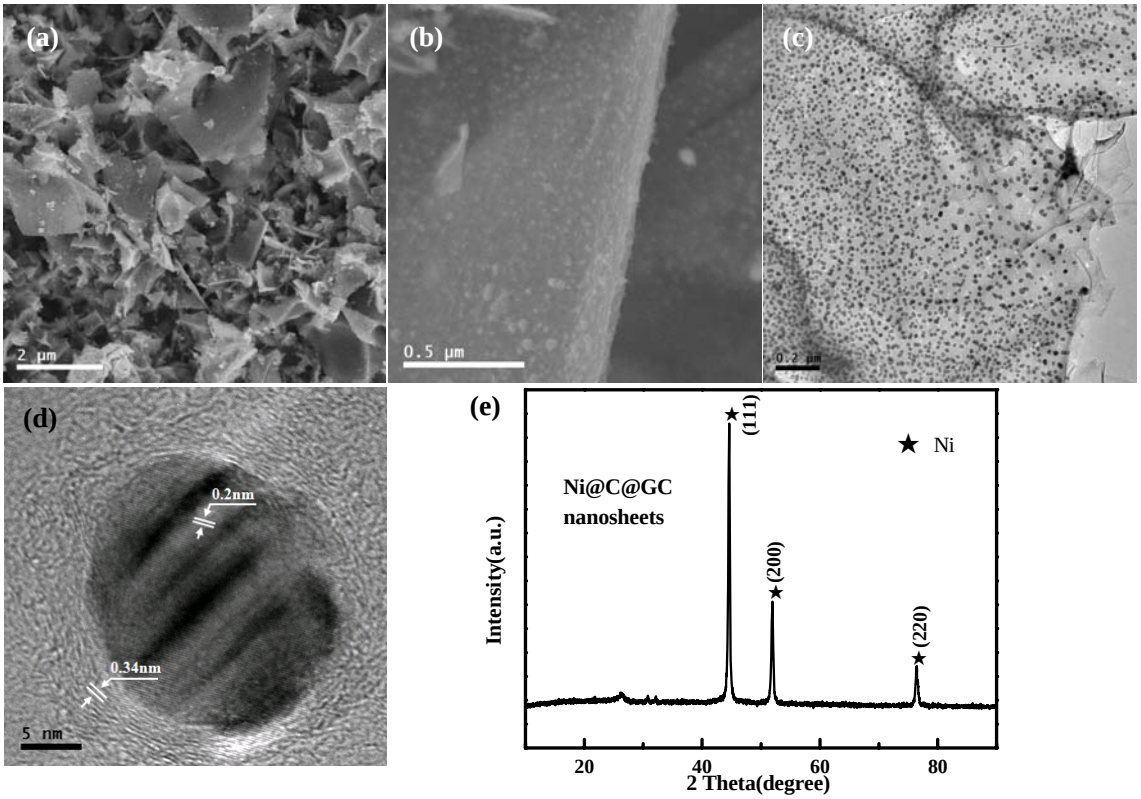

Figure S2. (a)-(b) SEM images of Ni@C@PGC nanosheets produced at 600 ^{o}C, (c)-(d) TEM and HRTEM images of Ni@C@PGC nanosheets produced at 600 ^{o}C, from which we can see that Ni particles coated with onion-like carbon shells (~2nm) were distributed evenly in the nanosheets without agglomeration. (d) XRD pattern of Ni@C@PGC nanosheets, illustrating that $Ni(NO_3)_2$ was reduced to Ni completely

before the CVT process.

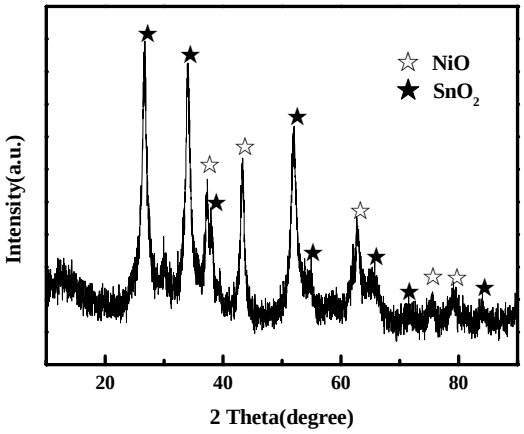

Figure S3. XRD pattern of Ni_3Sn_2@C@PGC after TGA analysis, form which we can see that the Ni_3Sn_2 was oxidized completely.

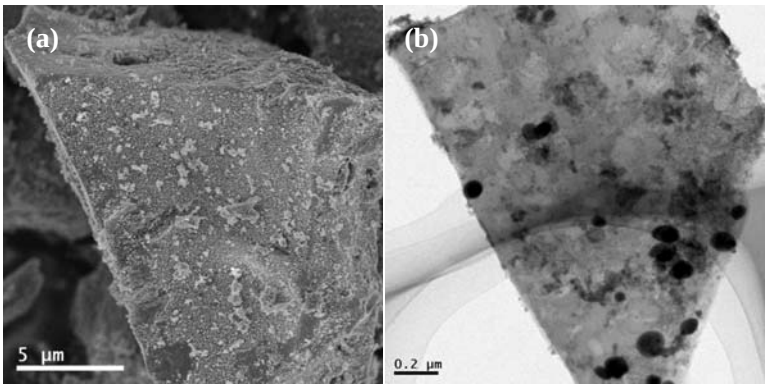

Figure S4. (a) SEM and (b) TEM image of Ni_3Sn_2/C nanoblock synthesized without using NaCl.

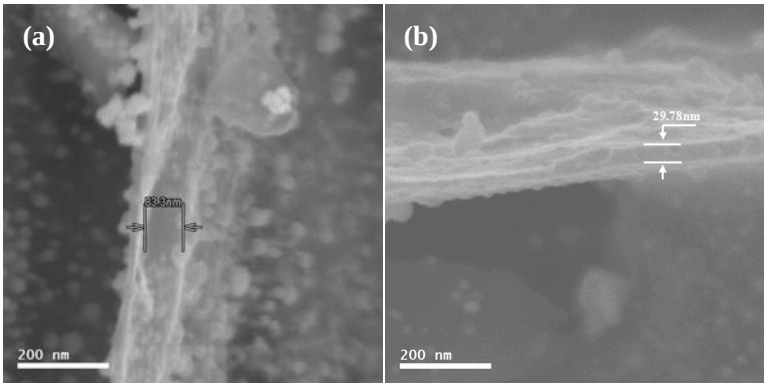

Figure S5. SEM images of 2D Ni_3Sn_2@C@PGC nanosheets, (a) W_{NaCl} : $W_{citric\ acid}$ = 2.94 : 1, in precursor, (b) W_{NaCl} : $W_{citric\ acid}$ = 5.88 : 1, in precursor. We can see that the thickness of 2D nanosheets can be adjusted by the amount of NaCl in precursor.

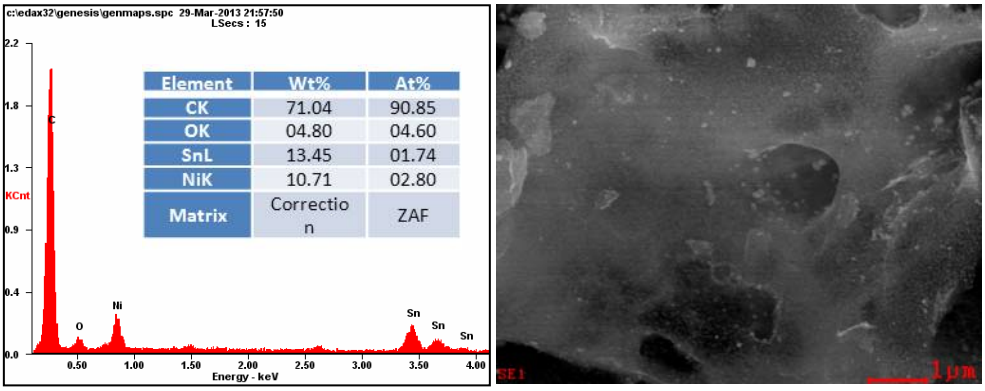

Figure S6. EDS spectrum of 2D Ni_3Sn_2@C@PGC nanosheets, showing that Ni : Sn (At%)≈3:2.

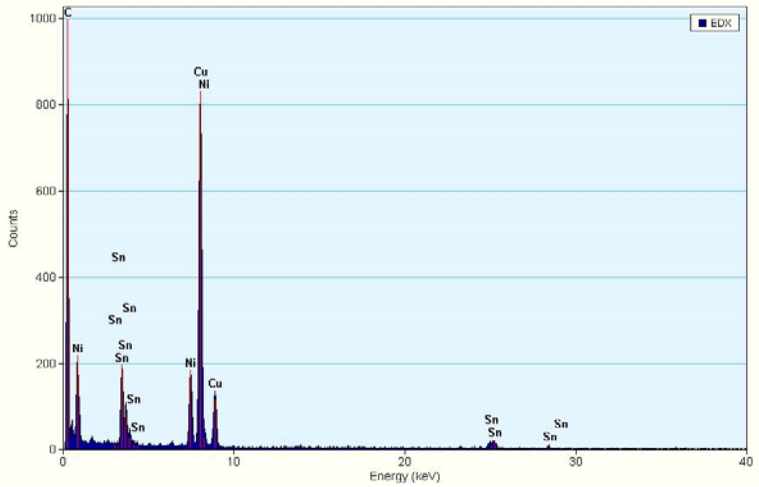

Figure S7. EDX spectrum of 2D Ni_3Sn_2@C@PGC nanosheets.

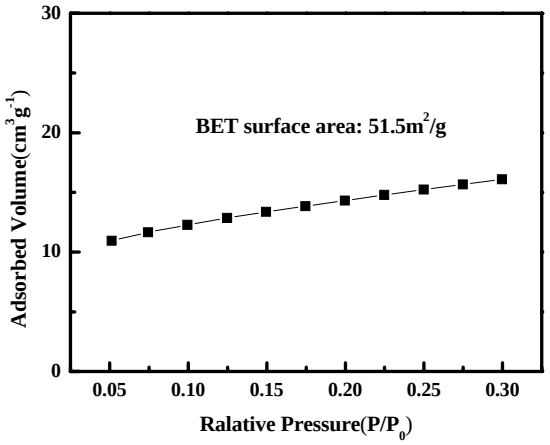

Figure S8. N_2 adsorption-desorption isotherms of Ni_3Sn_2/C nanoblocks, suggesting that their BET surface area is much lower than that of 2D Ni_3Sn_2@C@PGC nanosheets.

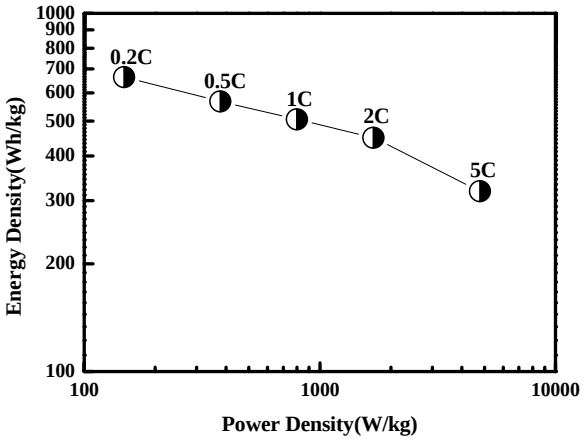

Figure S9. Ragone plot exhibiting the power density and energy density of 2D Ni_3Sn_2@C@PGC hybrid electrode.

Table S1. Detailed information of rate cycle performance of 2D Ni_3Sn_2@C@PGC nanosheet and Ni_3Sn_2/C nanoblock electrodes corresponding to Figure 5d.

Rate cycle number	Step number	Cycle number	Charge/discharge rate (C, 1C = 570 mAh/g)	Average reversible capacity of 2D Ni_3Sn_2@C@PGC electrode (mAh/g)	Average reversible capacity of Ni_3Sn_2/C nanoblocks electrode (mAh/g)
1	1	30	0.2	489	121.8
	2	60	0.5	424.7	88.1
	3	90	1	372	64.2
	4	120	2	313.6	44.2
	5	150	5	190.8	23.9
2	6	180	0.2	500.3	140.9
	7	210	0.5	427.7	
	8	240	1	325.8	
	9	270	2	194.9	
	10	300	5	61.7	
	11	320	0.2	481.5	